Proceedings of the 10th Australasian Heat and Mass Transfer Conference (AHMT2016), Brisbane, Australia, July 14-15, 2016

Liquid-liquid slug flow for enhanced heat transfer

Thilaksiri Bandara [a*], Manu Chandrashekar [b], Nitin Karwa [c] and Gary Rosengarten [d]

School of Aerospace, Mechanical and Manufacturing Engineering, RMIT University, 115, Queensberry Street, Carlton, Victoria 3053, Australia

[a]p.m.thilaksiri.bandara@rmit.edu.au, [b]s3517687@student.rmit.edu.au, [c]nitin.karwa@rmit.edu.au, [d]gary.rosengarten@rmit.edu.au

Keywords: slug flow, heat transfer, Nusselt number, film thickness.

Abstract. Liquid-liquid slug flow in microchannels can increase the heat transfer rates due to the internal recirculation within the liquid slugs. This paper presents experimental studies of heat transfer enhancement in microchannels with liquid-liquid slug flow. The experimental studies are carried out using a stainless steel channel with a circular cross section. Water is used as the dispersed phase fluid while silicon oil is used as the primary phase. The channel is heated by Joule heating. Two-phase flow is formed using a T-junction of 1 mm circular channels made using PDMS, and a specific channel arrangement was designed in the outlet channel in order to avoid the flow disruption when introducing the flow to the steel tube. The flow visualization is carried out with a Phantom V1610 camera and flow is visualized at both before and after the steel tube to ensure the required flow is passing through the tube. Experimental results showed over 400% increase in heat transfer with liquid-liquid slug flow compared to its single phase counterpart.

Introduction

Two-phase slug flow in microchannels has a wide range of industrial applications. Some of these applications include heat exchangers, electronic cooling, micro-reactors, and lab-on-a-chip which require high heat and mass transfer enhancement. Slug flow, which involves slugs of one phase distributed into a continuous phase, can produce a high rate of heat removal due to the internal recirculation within the liquid slugs and plug as shown in Fig. 1. This type of flow is also named as Taylor flow when there is a thin film around the liquid plug.

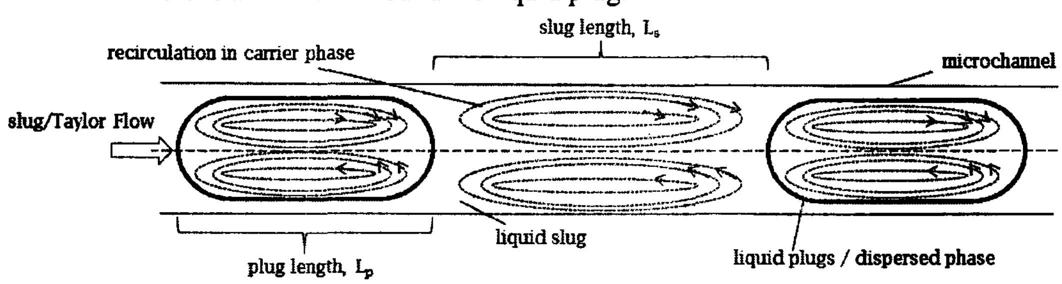

Fig 1. Schematic diagram of a slug flow

Earliest studies on heat transfer in slug flow includes Oliver and Wright [1] and Oliver and Young Hoon [2]. However, these studies were on gas-liquid two-phase flow. Since then, a significant amount of research work has been carried out on gas-liquid slug flow as discussed extensively in our recent review paper [3].

Even though gas-liquid two-phase flow has large impact on heat removal there are drawbacks and limitations. The introduction of immiscible liquid-droplets with higher heat capacity and conductivity has the potential to overcome these problem. There is a considerable amount of studies on hydrodynamics of liquid-liquid slug flow in microchannels [3]. While heat transfer during slug flow in microchannels has been studied numerically, there has been only a few experimental studies to date. Asthana et al. [4] experimentally investigated the heat transfer enhancement in microchannels with liquid-liquid two-phase flow. They investigated the effect of slug size on heat transfer, showing increased droplet size yields more efficient heat transfer and higher values of Nusselt number (Nu).

Recent experimental studies carried out by Eain et al. [5] investigated the Taylor flow heat transfer in a stainless steel tube with a three different oil/water combinations. They reported up to 600% increase of Nu over single phase flow due to the introduction of second immiscible phase with the shortest slug and longest plug lengths. A significant effect of film thickness on heat transfer was also found in their experiments. Increasing film thickness causes for poor heat transfer rates and hence lower Nusselt numbers.

The most recent study by Dai et al. [6] examined the flow and heat transfer behaviour of liquid-liquid slug flow by performing both experiments and CFD simulations for 1 and 2 mm vertical tubes with constant wall heat flux boundary conditions. They showed that heat transfer coefficients in slug flow are extremely sensitive to experimental uncertainties, but overall showed a good agreement between experiments and simulations. They also highlighted the difficulty in liquid-liquid heat transfer measurements due to the large uncertainties caused from high sensitivity of Nusselt number calculations to small differences in flow velocity.

Although there have been previous studies on both experimental and numerical studies on two-phase slug flow and associated heat transfer phenomena, liquid-liquid slug flow has been given very little attention in the literature. Thus, the aim of the present study is to investigate the heat transfer enhancement in microchannels with oil-water slug flow. This paper will present some important findings on liquid-liquid slug flow heat transfer in microchannels.

Experimental set up and procedures

A heat transfer apparatus with a 1 mm ID stainless steel tube was set up as shown in Fig. 2. The stainless steel tube was heated with Joule heating creating a constant wall heat flux boundary condition. However, the drawback in using a steel tube is that the flow cannot be visualised while the heat transfer experiments are running. Visualisation is required to determine flow parameters (slug lengths and plug lengths etc.,) as the primary objective of the study to analyse heat transfer with different slug flow parameters. Therefore, a special arrangement was used in order to visualise the flow before entering to the stainless steel tube.

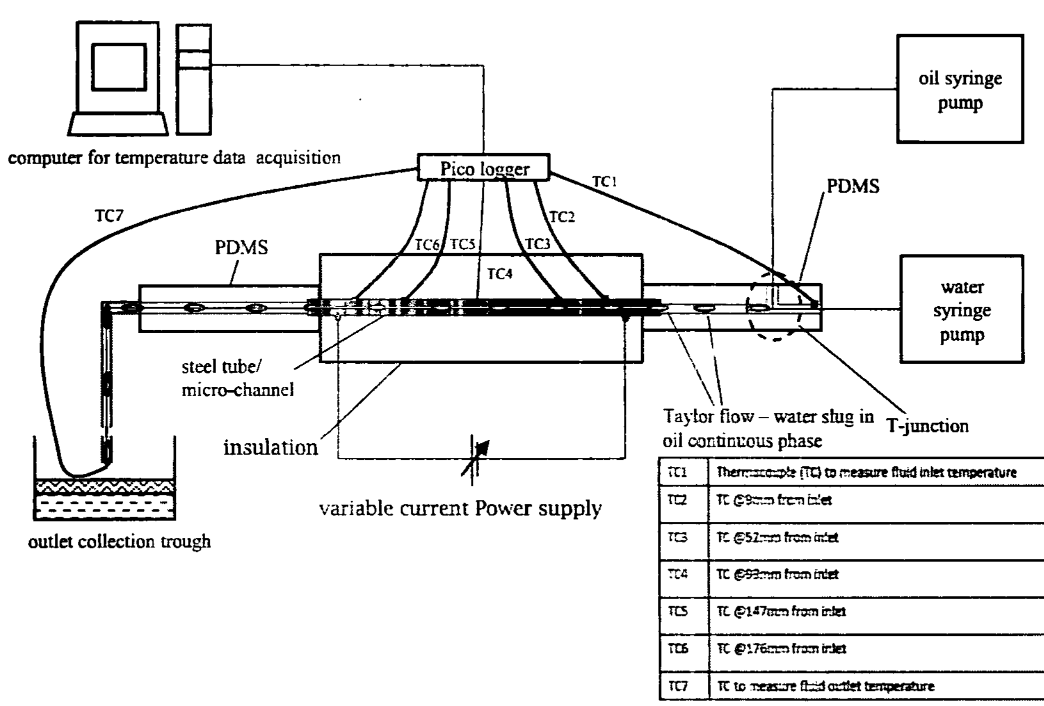

Fig. 2 Schematic diagram of experimental set up for heat transfer study

The length of the steel channel (density, ρ=8000 kg/m^3, specific heat, c_p = 500 J/kg K, and thermal conductivity, k = 16 W/m K) is 200 mm while a length of 190 mm is heated with Joule heating and 5 mm from each side is left for fitting the tubing. Two wires were connected to two copper rings which were silver soldered to the tube for supplying power. These wires were also silver soldered to two rings. Silver soldering minimises the contact resistance, meaning a uniform wall heat flux could be maintained using an ISO-Tech programmable DC power supply. The experimental set up is validated using single phase flow heat transfer. Liquid-liquid slug flow is generated using water ρ =998 kg/m^3, c_p = 4182 J/kg K, and k = 0.6 W/m K) and 1.5 cSt silicon oil (ρ =853 kg/m^3, c_p = 1800 J/kg K, and k = 0.1047 W/m K) as the working fluids. The interfacial tension between the silicon oil and water is 36.5 mN/m [7]. The viscosities of the two fluids changing significantly with temperature. Therefore, viscosity values were calculated as temperature dependent values during the heat transfer analysis section using $\mu_w(T) = 0.0000002T^2 - 0.00003T + 0.0015$ for water and $\mu_o(T) = 0.00000001T^2 - 0.00002T + 0.0018$ for oil. Here, μ_w, μ_o and T are water viscosity, oil viscosity and temperature in °C respectively.

Slug flow generation

A T-junction made with Polydimethylsiloxane (PDMS) is used for flow visualisation and introduction the flow into the heat transfer test rig. A schematic diagram of the PDMS T-junction is given in Fig. 3 (b).

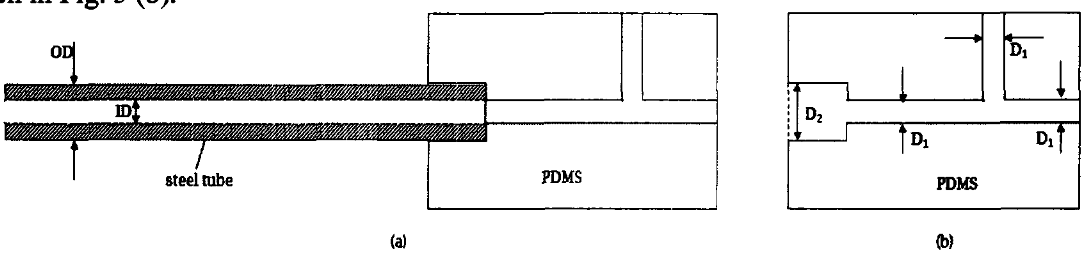

Fig.3 Detailed illustration of PDMS T-junction

In this T-junction, inlet and outlet channels were created with a diameter of 1 mm (D_1). However, slightly larger channel (diameter of D_2) which is equal to the outer diameter of the stainless steel tube (used for heat transfer study with 1 mm ID) is fabricated in order to connect the steel tube to the PDMS channel without a diameter change as shown in Fig. 3 (a). This ensures no flow disruptions due to diameter mismatching between the channels. The selection of material is an important step in designing droplet based microfluidics devices as the wall wettability plays a key role in slug flow formation. PDMS channels are hydrophobic for organic solvents such as water as discussed in [8]. Therefore, silicon oil was selected as the continuous phase. The Phantom V1610 high speed camera was used for flow visualization. The images obtained from the camera was analyzed frame-by-frame in order to obtain the sizes of the oil and water slug lengths. The images were captured at 16000 frames per second (fps) with 256 x 576 pixels. The images were recorded with a 4x magnification lens. The plug velocity (U_p), slug length (L_s) and plug length (L_p) were calculated by image analysis. Two different syringe pumps (Harvard apparatus PHD Ultra pump and KD Scientific infusion only pump) are used for flow formation for having different flow rate ratios accurately. A series of flow visualisation experiments were carried out before each heat transfer experiments and images were captured before and after the steel tube and compared. They gave a maximum variation of 10% for the slug and plug lengths.

Calculation of heat transfer

The amount of heat supplied via Joule heating to the channel (q) can be calculated as q = VI with known voltage (V) and current (I). The total heat flux on the channel wall can be calculated assuming the losses are negligible from the heating channel in the Styrofoam insulation box. Thus, the total heat flux on the inner wall of the channel is given by $q'' = q/\pi D_i L$. Here, D_i and L are inner diameter of the heated channel and the length of the channel respectively. Measuring inner wall and bulk fluid temperatures is challenging in microchannel heat transfer experiments while the outer wall temperature can be measured with fine thermocouple wires connected to outer wall. Therefore, one dimensional heat conduction is used for calculating the inner wall temperature at each location of the outer wall temperature measurement. The bulk fluid temperature at each thermocouple position is calculated by considering the energy balance method. The local convective heat transfer coefficient at a distance x is calculated using $h_x = q''/(T_{wix}-T_{mx})$. Here T_{wix} is inner wall temperature at an axial distance of x, and T_{mx} is bulk fluid temperature at that position. Hence, the local Nusselt number along the channel wall is calculated from $Nu_x = h_x D_i/k_f$, where k_f is the thermal conductivity of working fluid. An effective value for k_f is calculated using the volume fraction of two liquids in slug flow experiments. An average Nu is calculated from the calculated local Nusselt numbers. The uncertainty values associated with the experiment were calculated using the method proposed by Coleman and Steele in 1999 [9]. Uncertainty values are given in the table 1.

Table 1 Uncertainties associated with measured and derived variables

	Variable	Uncertainty
	flow rate	0.35 %
	channel diameter	±0.05 mm (5 %)
	channel length	±1 mm (0.5 %)
	temperature	±0.1°C (2.3 %)
Primary variable	material properties	3 %
	pixels	±1
	current	±0.01 A (3.3 %)
	voltage	±0.01 V (3.3 %)
	pressure	±7 Pa
	Reynold number	10.8 %
Derived variables	slug length	±1.6 μm
	Nusselt number	8.8 %

Results and discussion

Flow visualization

Flow rate ratio (primary phase fluid flow rate to secondary phase fluid flow rate, Q_p/Q_s) of two non-mixing fluids was the only controllable parameter in the present study as the other parameters such as dimensions of T-junction and the fluid properties were chosen to be fixed throughout the study. Therefore, a range of different flow rate ratios were chosen in order to get different slug lengths (L_s) and plug lengths (L_p). Some of the flow patterns are shown in Fig. 4.

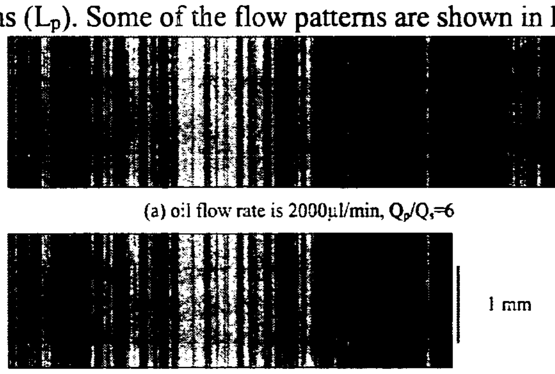

(a) oil flow rate is 2000μl/min, Q_p/Q_s=6

(b) oil flow rate is 2000μl/min, Q_p/Q_s=2.4

Fig. 4 Slug flow with 2000 μl/min constant oil flow rate

Heat Transfer

Single phase flow heat transfer

Initially single phase flow heat transfer experiments are carried out in order to validate the experimental set up. Experiments were carried out for Reynolds numbers (Re) from 10 to 295 for both water and oil as the working fluid. At steady state the overall heat balance for the heating system can be expressed as,

$$q_f = \dot{m}c_p(T_{out} - T_{in}) = q_{in} - q_{loss} \quad (1)$$

where $\dot{m}=\dot{Q}\rho$ is the mass flow rate. q_f, $\dot{Q}$, ρ, c_p, T_{in}, T_{out}, q_{in}, and q_{loss} are heat transferred to the fluid, volume flow rate, density of fluid, specific heat of fluid, inlet fluid temperature, outlet fluid temperature, power input from Joule heating and the heat loss to the ambient respectively. In general, the heat loss was very small due to the well-insulated experimental set up and this value was below 10% of the input power indicating the power was predominantly transferred to the fluid stream.

The bulk temperature should increase linearly along the channel for constant heat flux wall boundary condition. Variation of measured outside wall temperature and calculated inside channel wall and bulk fluid temperatures along the channel for a flow with total flow rate of 5000 µl/min is given in Fig. 5 (a).

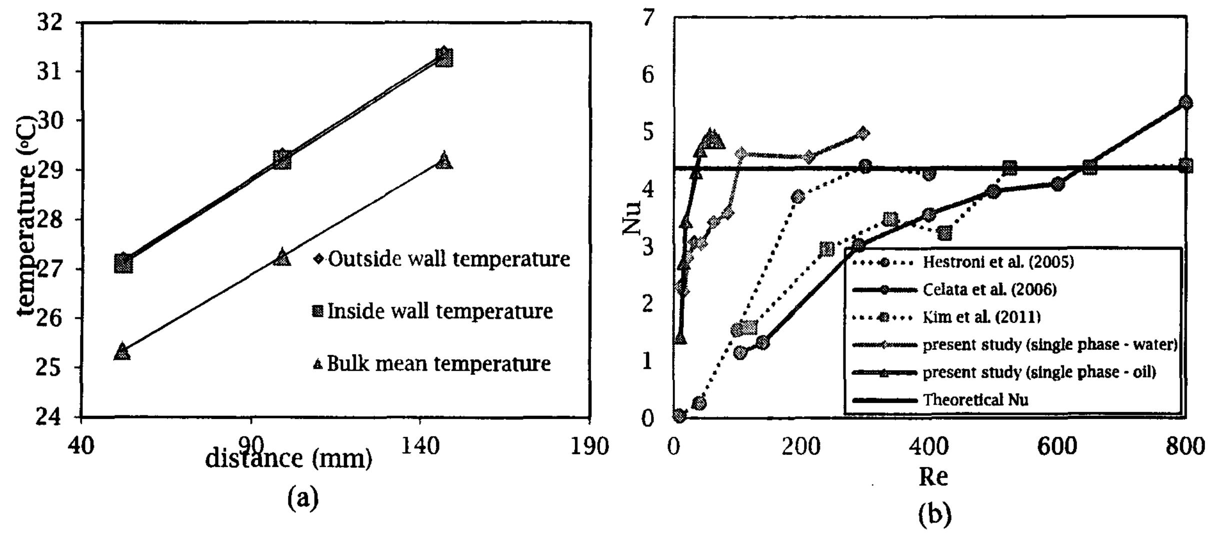

Fig. 5 (a) variation of outer wall, inner wall and bulk fluid temperature along the channel, (b) comparison of single phase flow Nu obtained from present study with experimental data from literature.

According to Fig. 5 (a) the temperatures vary linearly as explained previously and the temperature difference between outer and inner walls is very small due to the small thermal resistance of the stainless steel. However, at lower Re flows, this temperature variation is not completely linear along the channel due to the scaling effects such as axial conduction and viscous heating. The local Nusselt number along the channel wall is calculated from the measured and calculated temperatures together with power input as discussed previously. An average Nusselt number for different flow rates/Reynolds numbers can be calculated from those local Nu values. The variation of average Nu with Re is illustrated in Fig. 5 (b). The black line represents the theoretical single phase flow Nu for this particular boundary condition. The calculated Nu values at lower Reynolds numbers are little lower than the theoretically expected value of 4.36 independent on Re. This could be due to the axial conduction within the fluid at very low Re flows. Most of the previous studies showed lower Nu values at low Re, showing that scaling effect plays a key role in lower flow rate flows.

Slug flow heat transfer

The homogeneous flow model which considers the two-phase as a single-phase having average fluid properties that depend upon the mixture quality is used in slug flow heat transfer analysis. The bulk fluid temperature was calculated similar to single phase flow calculation using the energy balance. However, the fluid properties were calculated as effective values based on the volume fraction of each liquid in the mixture as given in the following equation.

$$X_{eff} = \phi X_s + (1 - \phi) X_p \qquad (2)$$

Here, X_{eff} is the effective value of property X. The subscripts p and s denote the primary and secondary fluid while ϕ is the volume fraction of secondary phase in the mixture. The local Nu values at different temperature measurement locations along the channel wall can be calculated using the above effective properties. Then an average Nusselt number for each flow combinations is calculated using the local Nu values along the channel. Fig. 6 (a) shows the calculated average Nu variation with Re for all the considered flow combinations within the study. The Nu is higher than the value of its single phase counterpart at each slug flow cases, showing the heat transfer enhancement due to the introduction of a secondary phase plugs. Nusselt number increases with Re up to a certain point and then it starts decreasing with increasing Re as shown in Fig. 6 (a). However, it is necessary to analyse the heat transfer rates against the flow parameters such as slug length, capillary number (Ca) and void fraction as only Re will not represent the state of the slug flow.

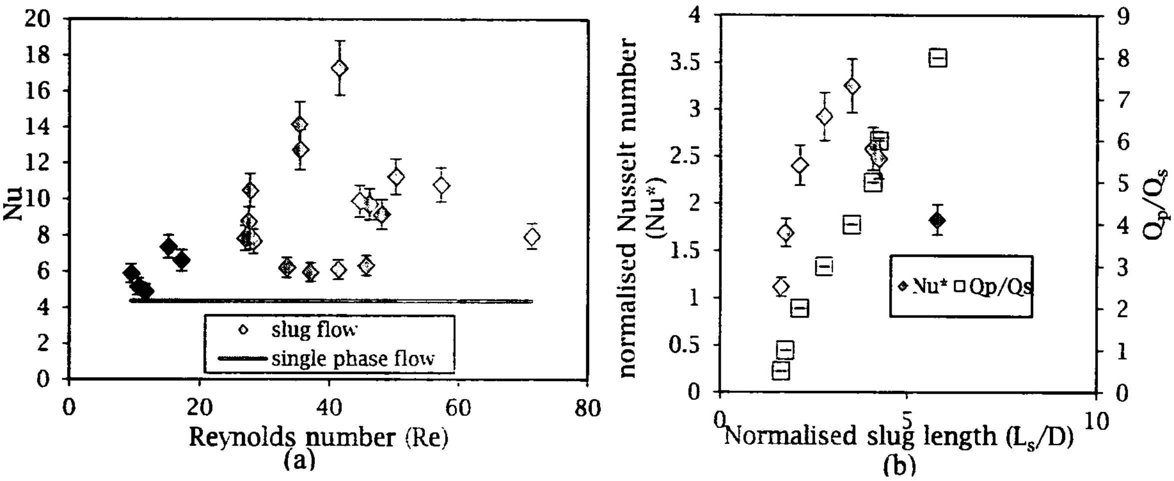

Fig. 6. (a) comparison of experimental slug flow Nu with theoretical single phase flow Nu, (b) variation of slug flow Nu (normalized with single phase flow Nu) with slug length, where water flow rate is a constant value of 500 µl/min.

Effect of slug and plug lengths on heat transfer

The normalised Nusselt number (ratio between two phase Nusselt number and single phase flow Nusselt number, $Nu^*=Nu_{tp}/Nu_{sp}$ variation with slug length is shown in Fig. 6 (b). The Nusselt number increases up to a certain slug length and then starts decreasing with further increase of slug length. The highest Nu was observed for the slug flow with $Qp/Q_s=3$ with total flow rate of 2000 µl/min. The numerical studies on effect of slug length on heat transfer showed that lower slug lengths give highest heat transfer rates [10]. Experimental results follow the same trend starting from 2.13 mm slug length which corresponds to the highest Nu which is 3.8 times higher than for single phase flow. Similar findings were reported on variation of Nu in gas-liquid two phase flow experiments in the literature [1, 2, 11, 12] with up to a 2.9 times (in [12]) higher than single phase flow.

Conclusions and future work

Experiments on slug flow were performed for flow visualisation and heat transfer studies. A steel channel with 1 mm internal diameter was used for heat transfer studies while the flow formation and visualisation were carried out on a PDMS T-junction. Water and 1.5 cSt silicon oil were used as the working fluids and silicon oil was selected as the primary fluid due to the wettability properties of PDMS. A wide range of liquid-liquid slug flow combinations were generated during the experiments and slug and plug lengths variation followed the similar trends reported in the literature.

Heat transfer under constant wall heat flux was studied experimentally for both single phase and slug flow. Single phase flow Nusselt numbers showed a good agreement with the theoretical value for this particular boundary conditions except little lower values at low Reynolds numbers. The slug flow heat transfer was carried out for different flow combinations in order to study the effect of slug length and a significant increase of Nu (up to 400%) was observed during the study. The heat transfer rates were analysed with slug and plug lengths and they showed a huge impact on heat transfer. The future work will include investigation of effect of other flow parameters such as void fraction, Ca and film thickness on heat transfer and developing correlations to accurately predict heat transfer on liquid-liquid slug flow.

References

[1] D. Oliver, S. Wright, Pressure drop and the heat transfer in gas-liquid two phase flow in horizontal tubes, Br. Chem. Eng. 9 (1964) 590-596.

[2] D. Oliver, A. Young Hoon, Two-phase non-Newtonian flow: Part 2 heat transfer, Trans. Inst. Chem. Eng., 46 (1968), 116-122.

[3] T. Bandara, N.-T. Nguyen, G. Rosengarten, Slug flow heat transfer without phase change in microchannels: a review, Chem. Eng. Sci., 126 (2015), 283-295.

[4] A. Asthana, I. Zinovik, C. Weinmueller, D. Poulikakos, Significant nusselt number increase in microchannels with a segmented flow of two immiscible liquids: An experimental study, Int. J. Heat Mass Transfer, 54 (2011), 1456-1464.

[5] M. M. G. Eain, V. Egan, J. Punch, Local nusselt number enhancements in liquid-liquid Taylor flow, Int. J. Multiphase flow, 80 (2015), 85-97.

[6] Z. Dai, Z. Guo, D. F. Fletcher, B. S. Haynes, Taylor flow in microchannels-unification of liquid-liquid and gas-liquid results, Chem. Eng. Sci., 138 (2015), 140-152.

[7] G. Paik, V. K. Pamula, K. Chakrabarty, Thermal effects on droplet transport in digital microfluidics with applications to chip cooling in : Thermal and Thermomechanical Phenomena in Electronic Systems, ITHERM 04, The ninth Intersociety conference on IEEE, (2004), 694-654.

[8] G. Christopher, S. Anna, Microfluidics methods for generating continuous droplet streams, J. Phys. D: App. Phys., 40 (2007), 140-152.

[9] H.W. Coleman, W. G. Steele, Experimentation, validation, and uncertainty analysis for engineers, John Wiley & Sons, (2009).

[10] T. Bandara, S. C. Cheung, G. Rosengarten, Slug flow heat transfer in microchannels: A numerical study, Comp. Thermal Sciences, 7 (2015), 81-92.

[11] P. Walsh, E. Walsh, Y. Muzychka, Heat transfer model for gas-liquid slug flows under constant flux, Int. J. Heat Mass Transfer, 53 (2010), 3293-3201.

[12] S. Leung, Y. Liu, D. F. Fletcher, B. S. Haynes, Heat transfer in well-characterised Taylor flow, Chem. Eng. Sci., 138 (2015), 140-152.